Modelling gas flow in a direct injection diesel engine: I – Squish and swirl

A. C. Hansen*

(Received February 1991)

Abstract

The objectives of this study were to formulate a less empirically based quasi-dimensional model which accounted for the gas flow characteristics of squish and swirl in a direct injection diesel engine and to verify the model with existing data. The model incorporates sub-models for generating in-cylinder gas flow components of squish and swirl at each crank angle between inlet valve closing and exhaust valve opening. Calibration and verification of the gas flow sub-models necessitated the use of published data. Good agreement was obtained between the present model and the experimental data from three engines, two with a bowl-in-piston and the other with a flat piston.

Introduction

In-cylinder air motion in diesel engines plays a major role in the combustion process and in heat transfer. Owing to the non-stationary character of this air motion caused by the reciprocating piston movement, analysis of the flow processes is complex. The application of the Navier-Stokes equations to these flow processes and the generation of a satisfactory solution on a three-dimensional basis requires not only considerable computer resources but also experimental data to verify such solutions. Arcoumanis and Whitelaw [1] stated that to achieve a totally predictive ability either the numerical methods had to be improved so that computing time was greatly reduced or computers with much larger storage capacity and speed had to emerge. It has been acknowledged by a number of researchers that model development has overtaken the availability of appropriate data to verify the output of these models. Hence there is still a fairly heavy reliance on empirically based models with the inclusion of physically related phenomena where possible.

In spite of these complexities of air motion the flow models that are presently applied provide results which correspond remarkably well with the experimental data that are available. The flow patterns are normally divided into mean flow components and fluctuating flow components, the latter being termed turbulence. High speed direct injection diesel engines rely heavily on swirl and squish as flow mechanisms for mixing the injected fuel with air. The interaction of these two mean flow components is also important during the compression and expansion strokes as high swirl may inhibit squish induced flow leading to less effective mixing [1].

The objectives of this study were to formulate a suitable model which accounted for the gas flow characteristics of squish and swirl in a direct injection diesel engine on a quasi-dimensional basis and to verify the model with existing data.

Formulation of model

The gas flow characteristics in the combustion chamber of a direct injection (DI) diesel engine during the compression and expansion strokes are governed primarily by piston velocity, squish, swirl and turbulence intensity. The variation of squish and swirl during the cycle is determined by the conservation of mass and angular momentum.

Squish Flow

The calculation of squish flow was carried out by assuming that the combustion chamber was divided into two volumes as shown in Figure 1. Following on the approach of Murakami, Arai and Hiroyasu [2], if the gas density ρ_c is regarded as uniform in the combustion chamber, then it can be shown that the mass transportation dm_1 from volume 2 to volume 1 relative to the movement of the piston dl is given by:

$$dm_1 = \frac{R_1^2.(R_1^2 - R_2^2)}{(R_1^2.h + R_2^2.1)^2}.h.m_o.dl \qquad (1)$$

where

m_o = total mass of charge in chamber, kg
h = depth of bowl in piston, m
l = instantaneous distance between top of piston and head, m
R_1 = radius of bowl, m
R_2 = radius of cylinder, m

The ratio of mass to volume in the inner volume is given by the charge density and hence:

$$\frac{dm_1}{dt} = \rho_c.\frac{dV_1}{dt} = \rho_c.A_{12}.\frac{dr}{dt} \qquad (2)$$

where

A_{12} = area of interface between volumes 1 and 2, m^2
$= 2\pi R_1.1$
dr/dt = radial or squish velocity, m/s

*Senior Lecturer, Department of Agricultural Engineering, University of Natal, Pietermaritzburg.

However,

$$\frac{dm_1}{dt} = \frac{dm_1}{dl}.\frac{dl}{dt} \qquad (3)$$

where

dl/dt = piston velocity, m/s.

Hence by combining equations (2) and (3), the squish velocity is given by:

$$\frac{dr}{dt} = \frac{1}{2\pi\rho_c.R_1.l}.\frac{dm_1}{dl}.\frac{dl}{dt} \qquad (4)$$

Using equations (1) and (4), the squish and reverse squish velocities can be calculated at any crank angle during the compresion and expansion strokes.

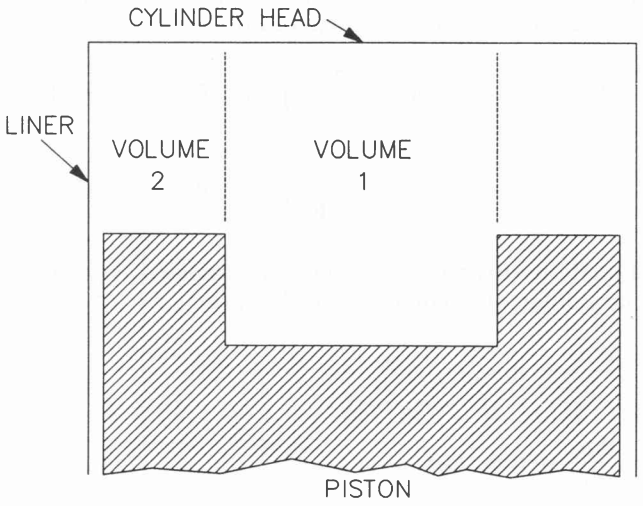

Figure 1 – Division of the combustion chamber for calculation of the squish velocity into the piston bowl

Axial flow into the cup resulting from the squish effect can be computed in a similar manner assuming a uniform air density. The chamber is divided into two volumes 3 and 4 as shown in Figure 2.

The mass transportation dm_4 from volume 3 to 4 relative to the movement of the piston dl is given by:

$$dm_4 = -\frac{R_1^2.R_2^2}{(R_2^2.l + R_1^2.h)^2}.h.m_o.dl$$

Applying the same approach as in equations (2) and (3) it then follows that the axial velocity into the bowl:

$$\frac{dx}{dt} = -\frac{R_2^2}{\pi\gamma^c(R_2^2.l + R_1^2.h)^2}.h.m_o.\frac{dl}{dt} \qquad (5)$$

Both the squish velocity from equation (4) and the axial velocity from equation (5) can be used as velocity components for computing resultant gas velocities in the combustion chamber. Equations (2) and (4) are also required in the calculation of swirl velocities.

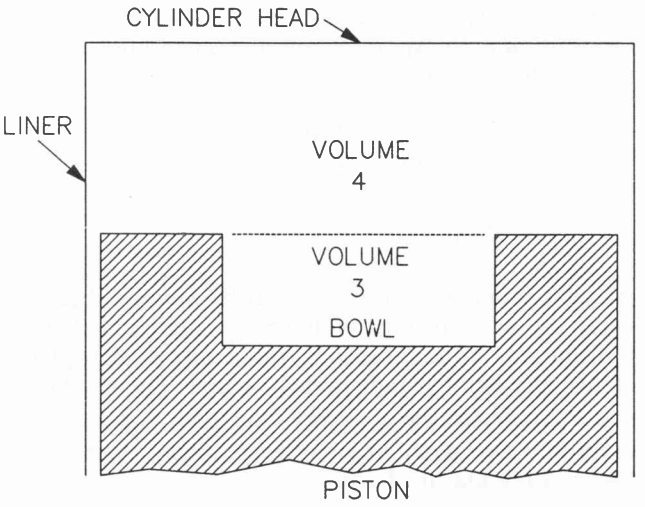

Figure 2 – Division of the combustion chamber for calculation of the axial velocity into the piston bowl.

Swirl Flow

The method selected for computing swirl flow is based on the model presented by Murakami *et al.* [2]. As for the squish flow calculation the combustion chamber is divided into an inner cylindrical volume 1 and an outer annular volume 2 by a virtual boundary radius equal to the bowl radius. The wall friction moment in each volume and the angular momentum exchange between the volumes provides the solution for the rotational speed of each volume ω_1 and ω_2.

According to Murakami *et al.* [2] if the variation of the angular momentum in each volume with respect to time is equal to the summation of the angular momentum exchange between the volumes and the wall friction moment in each volume, then:

$$\frac{d(I_1\omega_1)}{dt} = T_{f1} + T_{f2} + T_{f6} + T_{v21} + T_{s21} \qquad (6)$$

$$\frac{d(I_2\omega_2)}{dt} = T_{f3} + T_{f4} + T_{f5} - T_{v21} - T_{s21} \qquad (7)$$

where I_1 = moment of inertia of inner volume
I_2 = moment of inertia of outer volume
T_{s21} = angular momentum flux transported from the inner volume to the outer volume by squish flow
T_{v21} = angular momentum flux transmitted from the inner volume to the outer volume by viscous shear
$T_{f1} - T_{f6}$ = wall friction moments for each of the six surfaces designated in Figure 1.

During the compression stroke, $dm_1 \geq 0$ and the angular momentum transportation from the outer to the inner volume is given by:

$$T_{s21} = -\omega_2.\frac{dI_2}{dt} = \frac{1}{2}.\frac{R_2^4 - R_1^4}{R_2^2 - R_1^2}.\omega_2.\frac{dm_1}{dt}$$

where $I_2 = \frac{1}{2}.\frac{R_2^4 - R_1^4}{R_2^2 - R_1^2}.m_2$

During the expansion stroke, $dm_1 < 0$ and the angular momentum is transported from the inner volume to the outer volume. Hence:

$$T_{s21} = \omega_1 . \frac{dI_1}{dt} = \frac{1}{2} . R_1^2 . \omega_1 . \frac{dm_1}{dt}$$

where $I_1 = \frac{1}{2} . R_1^2 . m_1$

Angular momentum transmission by viscous shear between the inner and outer volumes was represented by the transmitted torque between two co-axial cylinders placed at the representative radii in each volume. These radii, R_{r1} and R_{r2} reflected the division of the inner and outer volumes into two equal volumes respectively as shown in Figure 3 [2]. On this basis:

$$T_{v21} = 4\pi\mu_e . 1 . \frac{R_{r2}^2 . R_{r1}^2}{R_{r2}^2 - R_{r1}^2} . (\omega_2 - \omega_1)$$

$$\mu_e = v_e . \rho_c$$
$$v_e = k^{0,5} . l_m$$
$$l_m = 0,14\ R_2/2$$
$$k = 0,74\ C_m^2$$

where μ_e = effective turbulent viscosity, Pa.s
v_e = effective turbulent kinematic viscosity, m^2/s
l_m = turbulence mixing length, m
k = turbulence kinetic energy, m^2/s^2
C_m = mean piston speed, m/s.

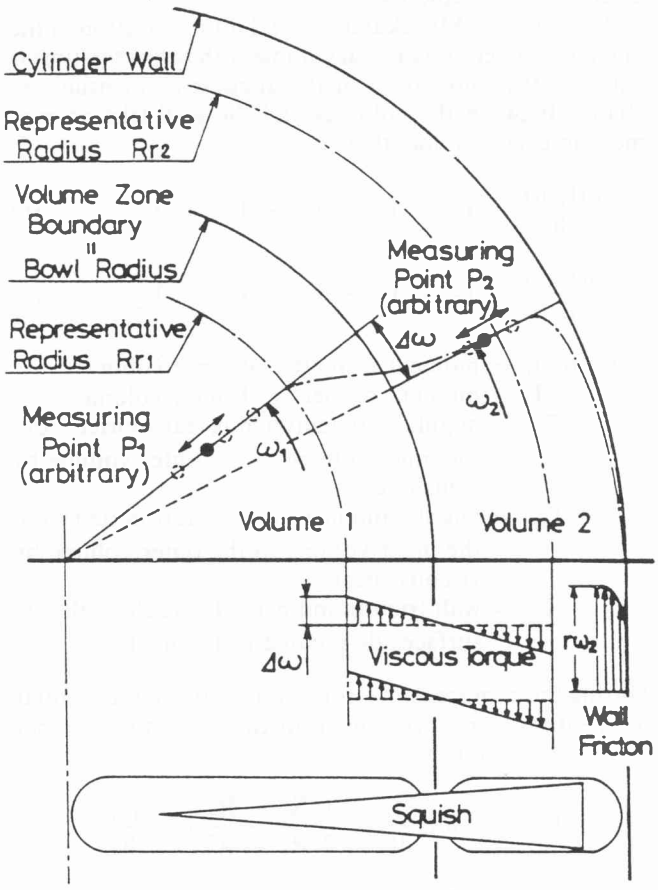

Figure 3 – Schematic of the terms and representative radii in each volume used in the model [2].

Murakami *et al.* [2] pointed out the difficulty of obtaining wall friction directly in the combustion chamber with its complex boundaries. The wall friction at each surface was therefore estimated by assuming an infinite atmosphere adjacent to each surface and then multiplying by a corrective coefficient, β. The friction moments on the disc-like surfaces were given by von Kármán's approximate solution. Hence:

$$T_{f1} = T_{f6} = \beta . (-0,0365) . \rho_c . \omega_1^2 . R_1^5 . \left(\frac{v}{\omega_1 . R_2^2}\right)^{0,2}$$

$$T_{f3} = T_{f5} = \beta . (-0,0365) . \rho_c . \omega_2^2 . \left\{R_2^5 \left(\frac{v}{\omega_2 . R_2^2}\right)^{0,2} - R_1^5 \left(\frac{v}{\omega_1 . R_2^2}\right)^{0,2}\right\}$$

where v = laminar kinematic viscosity, m^2/s.

The friction moments on the cylindrical surfaces were provided by the local friction coefficient for a flat plate, thus giving the following equations:

$$T_{f2} = \beta . (-0,0296) . \left(\frac{2v}{\omega_1 . R_1^2}\right)^{0,2} . \rho_c . (R_1 . \omega_1)^2 . 2\pi R_1^2 h$$

$$T_{f4} = \beta . (-0,0296) . \left(\frac{2v}{\omega_2 . R_2^2}\right)^{0,2} . \rho_c . (R_2 . \omega_2)^2 . 2\pi R_2^2 l$$

Equations (6) and (7) can then be represented as two ordinary differential equations of the form:

$$\frac{d\omega_1}{dt} = f(\omega_1, \omega_2)$$

$$\frac{d\omega_2}{dt} = f(\omega_1, \omega_2)$$

These equations were treated as simultaneous equations and were solved by iteration at each crank angle increment using the predictor-corrector method. The solution was started with the Runga-Kutta method. Variables that were computed with each increment of crank rotation, and used in the equations, included the distance between piston crown and head, the mass of gas in each volume, the gas density and the kinematic viscosity of the gas.

Model calibration and verification

Three sets of published data were selected for calibrating and verifying the model. As the swirl and squish flow model was the same as applied by Murakami *et al.* [2] their data were used to check for errors that may have been made in implementing the relevant equations. The other sets of data used were those of Johnston, Robinson, Rorke, Smith and Witze [3] and Morel and Keribar [4]. A similar procedure to Morel and Keribar [4] was applied which often made use of the same equations and hence it was appropriate to compare model outputs where possible. The data of Johnston *et al.* [3] were used for verification of the model in the same way as Morel and Keribar [4].

Murakami *et al.* [2] presented graphs of angular momentum contributions from wall friction, from viscous shear between volumes and from squish flow between volumes. As indicated earlier they divided the chamber into two volumes consisting of an inner cylindrical volume of radius equal to the cup and an outer volume making up the remaining portion above the piston crown. the curves were generated for a standard piston configuration with a compression ratio of 13:1 and for an engine speed of 1 000 r/min. By adopting the same engine configuration and equations governing the flow characteristics excellent agreement with the swirl ratios of Murakami *et al.* [2] was obtained for both volumes as illustrated in Figure 4.

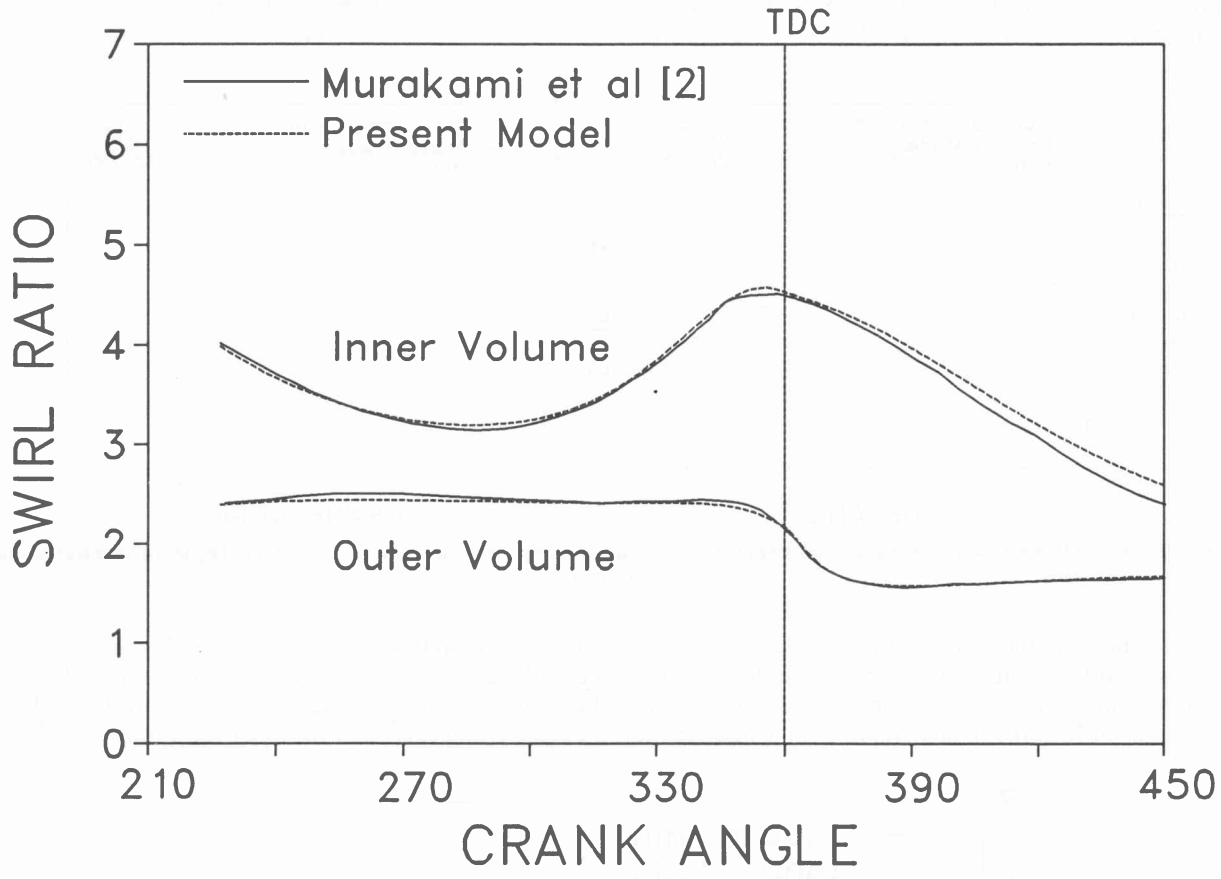

Figure 4 – Variation of swirl ratios compared to those of Murakami *et al.* [2] at 1 000 r/min.

The remaining small differences between curves in Figure 4 can be attributed to differences in assumed temperature and pressure conditions which affect the density and viscosity of the air in the chamber. As specified by Murakami *et al.* [2] the corrective coefficient β detailed earlier representing an adjustable friction factor was set equal to two for both the inner and outer volumes in generating the swirl ratios in Figure 4.

Having obtained good agreement with the results of Murakami *et al.* [2] the results of Morel and Keribar [4] were used as an independent check. The swirl equation applied by Morel and Keribar [4] also involved angular momentum changes but applied to three volumes instead of two. The inner volume specified by Murakami *et al.* [2] was divided further by Morel and Keribar [4] into a volume corresponding to the bowl and the volume above the bowl. The equations also took into account squish effects and viscous friction as well as intake and exchaust flux of angular momentum thus accounting for events during the intake and exhaust strokes in addition to compression and expansion.

Morel and Keribar [4] provided sets of graphs for one particular engine configuration and operating condition which was established as the baseline case. The engine modelled was a turbo – charged direct injection unit with a displacement of 2 L/cylinder operating at 1800 r/min and 1 517 kPa IMEP. The combustion chamber had a compression ratio of 14,8, bore/stroke ratio of 0,92 and piston cup diameter/bore ratio of 0,67. The cup contained 88% of the chamber volume at TDC.

Because of the difficulty of simulating the actual combustion and the resulting pressure development, comparisons were made with the data of Morel and Keribar [4] using data generated under motored conditions. The turbocharger on the baseline engine produced a bulk gas temperature, T_2 at IVC of 485 K. Assuming atmospheric air temperature, $T_1 = 25°C$, barometric pressure $P_1 = 100$ kPa and compressor efficiency $e_c = 60\%$ and applying the following equation from Goering [5]:

$$T_2/T_1 = 1 + [(P_1/P_2)^{0.286} - 1]/e_c,$$

the resulting inlet manifold pressure P_2 was approximately 300 kPa giving a pressure ratio of three. Bulk gas temperature was adjusted to be the same as the unburned zone temperature given by Morel and Keribar [4] in one of their graphs. All subsequent comparisons with the model of Morel and Keribar [4] were based on these values.

Apart from a small relative increase in cylinder mass from the injected fuel and changes in the viscosity of the chamber contents with the increased bulk gas temperatures from combustion, the gas velocity characteristics generated from the two models were expected to be comparable. Figure 5 shows the swirl ratios for the inner and outer volumes respectively for the two models.

The swirl ratios for the inner volume in figure 5 compare very favourably. The deviation close to TDC can be attributed to injection and combustion in the curve of Morel and Keribar [4]. The fuel injected before TDC increases the density of the chamber contents and hence the angular momentum transportation from the outer volume to the inner volume. This change increases the swirl velocity of the inner volume.

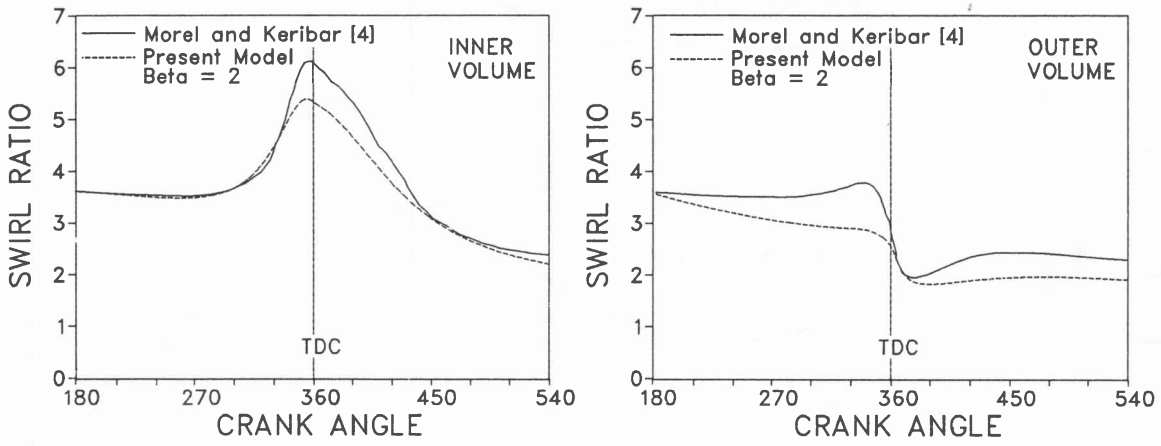

Figure 5 – Variation of swirl ratios with crank angle from the present model compared to the swirl ratios obtained by Morel and Keribar [4] at 1800 r/min.

The swirl ratios for the outer volume in Figure 5 differ substantially with the curve of the present model decaying at a marked rate. The increase in speed from 1 000 r/min for the engine of Murakami *et al.* [2] to 1 800 r/min for the engine of Morel and Keribar [4] was then examined as a possible factor contributing to the difference. However, Figure 6 shows that an increase in speed from 1 000 r/min to 1 800 r/min increases the swirl ratio only slightly.

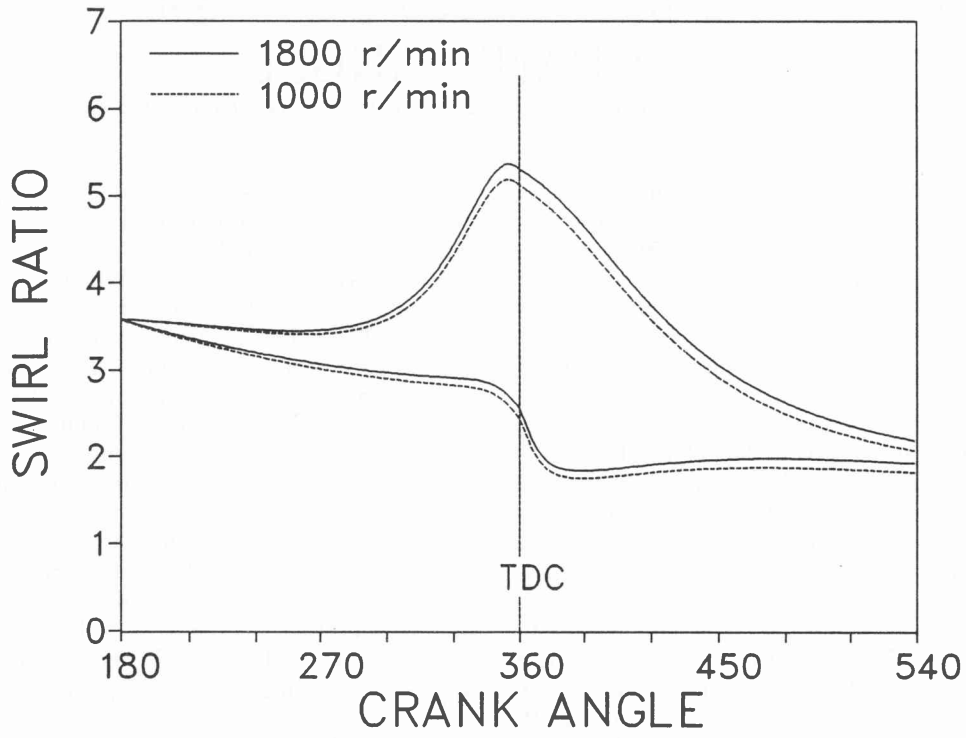

Figure 6 – Variation of swirl ratio in the inner and outer volumes for two different speeds applied to the baseline engine of Morel and Keribar [4].

The discrepancies in Figure 6 suggested that a different corrective coefficient for each volume should be examined. In order to determine a suitable β for the outer volume, the validation procedure used by Morel and Keribar [4] was adopted. They selected a set of measured data from Johnston *et al.* [3] that were obtained from an engine with pancake combustion chamber geometry and compression ratio of 5,4. The swirl ratio at 160 °BTDC was extremely high being 18,25 because of the tangential intake valve used. Morel and Keribar [4] stated that, because of the high initial swirl value, the percentage swirl decay during compression and expansion caused by wall friction would also be high, thus providing an ideal situation for model testing.

Morel and Keribar [4] computed the maximum tangential swirl velocity at the wall to represent the maximum velocity measured by Johnston *et al.* [3]. This value provided approximately equal initial momentum for the calculation and for the experiment. Figure 7 shows the swirl ratios generated by Morel and Keribar [4] compared to the experimental data of Johnston *et al.* [3]. In applying the present model to the same engine it was necessary to decide how to specify the inner and outer volumes for the flat piston arrangement. Murakami *et al* [2] found that, from the tangential velocity distribution obtained experimentally from a flat piston geometry, a boundary between the volumes could be drawn on the radii of 60% to 70% of cylinder radius. They subsequently used 65% for the flat piston arrangement in their work. Morel and Keribar [4] did not specify the boundary directly although for this particular verification they mentioned the assumption of a linear velocity profile increasing from zero at the centreline to a maximum at the wall.

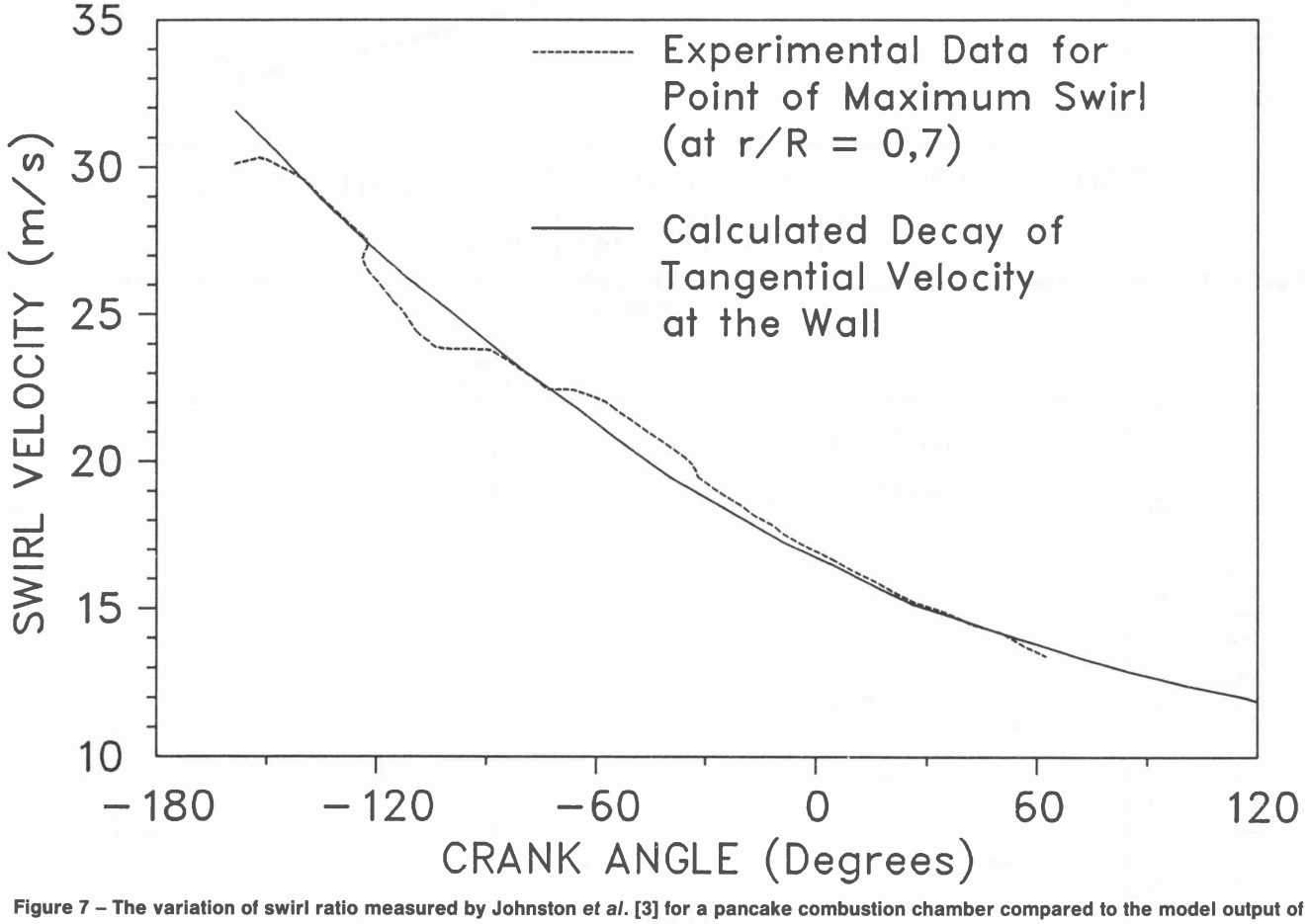

Figure 7 – The variation of swirl ratio measured by Johnston *et al.* [3] for a pancake combustion chamber compared to the model output of Morel and Keribar [4].

In keeping with the recommendations of Murakami *et al.* [2] a boundary at 65% of cylinder radius was used to generate the swirl velocity in the present model for the engine of Johnston *et al.* [3]. Figure 8 shows the curve published by Morel and Keribar [4] and the curves generated by the present model. The corrective coefficient β was initially set equal to two and then decreased to one to reduce the viscous torque. The latter setting provided results which corresponded fairly closely to the curve of Morel and Keribar [4] and hence to the measured data of Johnston *et al.* [3].

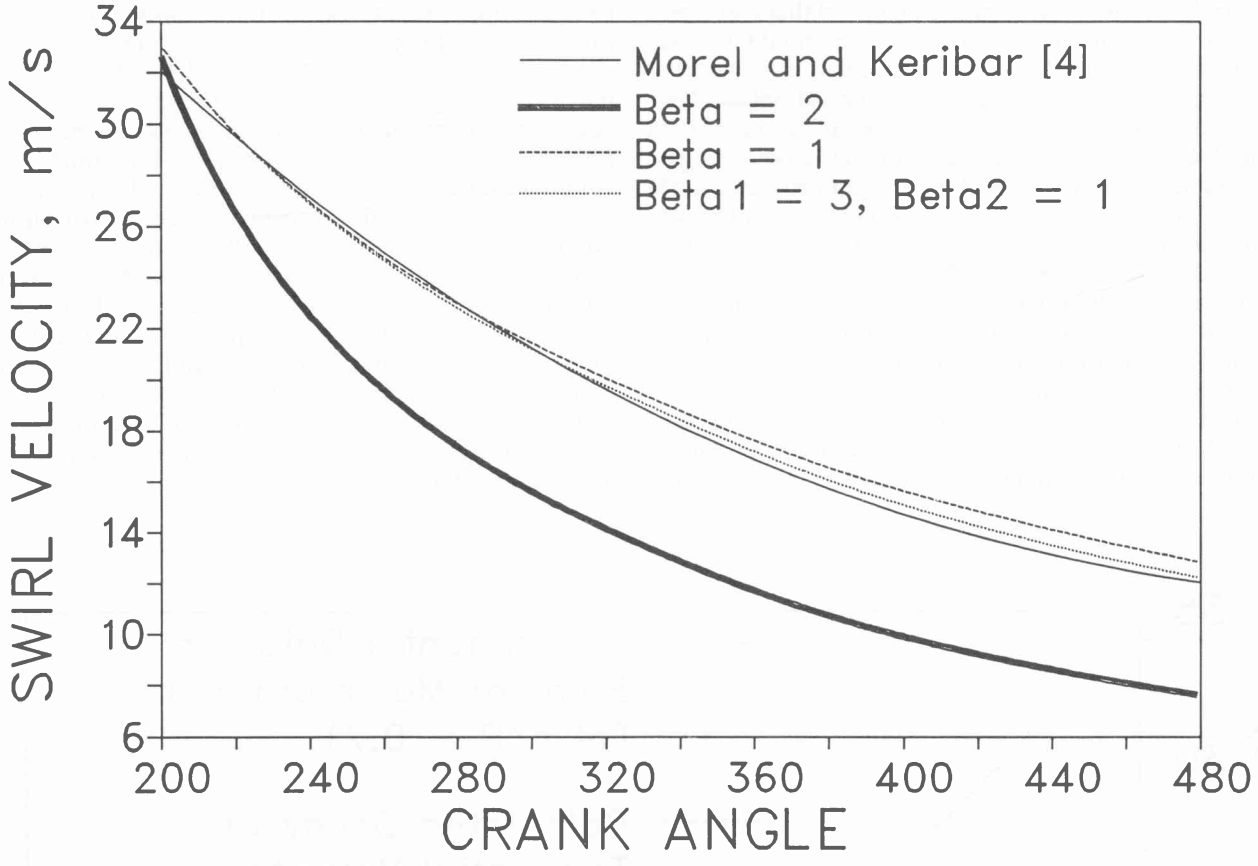

Figure 8 – The swirl ratios from the present model with different convective coefficients applied to the engine of Johnston *et al.* [3] compared to the model output of Morel and Keribar. [4].

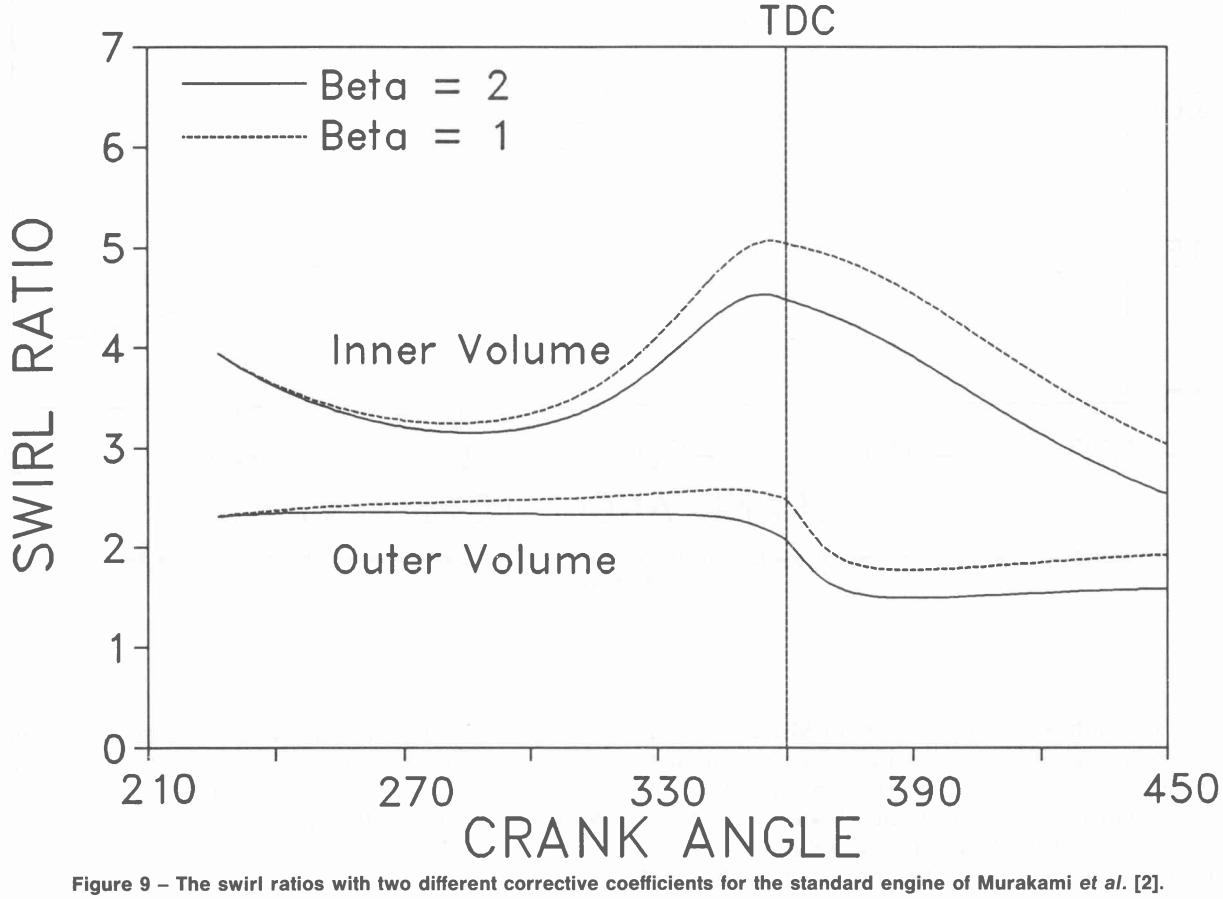

Figure 9 – The swirl ratios with two different corrective coefficients for the standard engine of Murakami *et al.* [2].

Murakami *et al.* [2] had achieved good agreement between their model and experimental data using $\beta = 2$. Decreasing β to one resulted in a substantial increase in swirl ratio for both volumes because of the effective decrease in wall friction as shown in Figure 9. A comparison with the curves of Morel and Keribar [4] using $\beta = 1$ showed much better agreement with the outer volume angular velocity but poor agreement with the inner volume. The effect of using different corrective coefficients for each volume was then investigated. Murakami *et al.* [2] concluded that for the inner volume, the value of β lay between 0 and 1 while for the outer volume the range was 2 to 4. This latter range specification contradicted the measured swirl values of Johnston *et al.* [3]. It also appeared that, in order to offset the higher swirl ratio of the inner volume a larger β was required implying a greater wall friction. Figure 10 shows the effect of specifying $\beta_1 = 3$ for the inner volume and $\beta_2 = 1$ for the outer volume. Apart from a slightly higher swirl ratio at the peak for the inner volume the curves follow very closely.

In the case of the outer volume there is some deviation over most of the compression and expansion strokes. The deviation is a maximum close to TDC, however, Murakami *et al.* [2] were not able to record data close to TDC to validate this section of the model. A direct comparison of this new curve with the experimental data suggests reasonable agreement.

Application of the same values of β_1 and β_2 to the flat piston engine of Johnston *et al.* [3] provided a curve in much closer agreement with the curve of Morel and Keribar [4] as shown earlier in Figure 8. Applying $\beta_1 = 3$ and $\beta_2 = 1$ to the engine of Morel and Keribar [4] yielded the curves shown in Figure 11. Once again fairly good agreement was achieved and it was concluded that the values of $\beta_1 = 3$ for the inner volume and $\beta_2 = 1$ for the outer volume should be used for further applications.

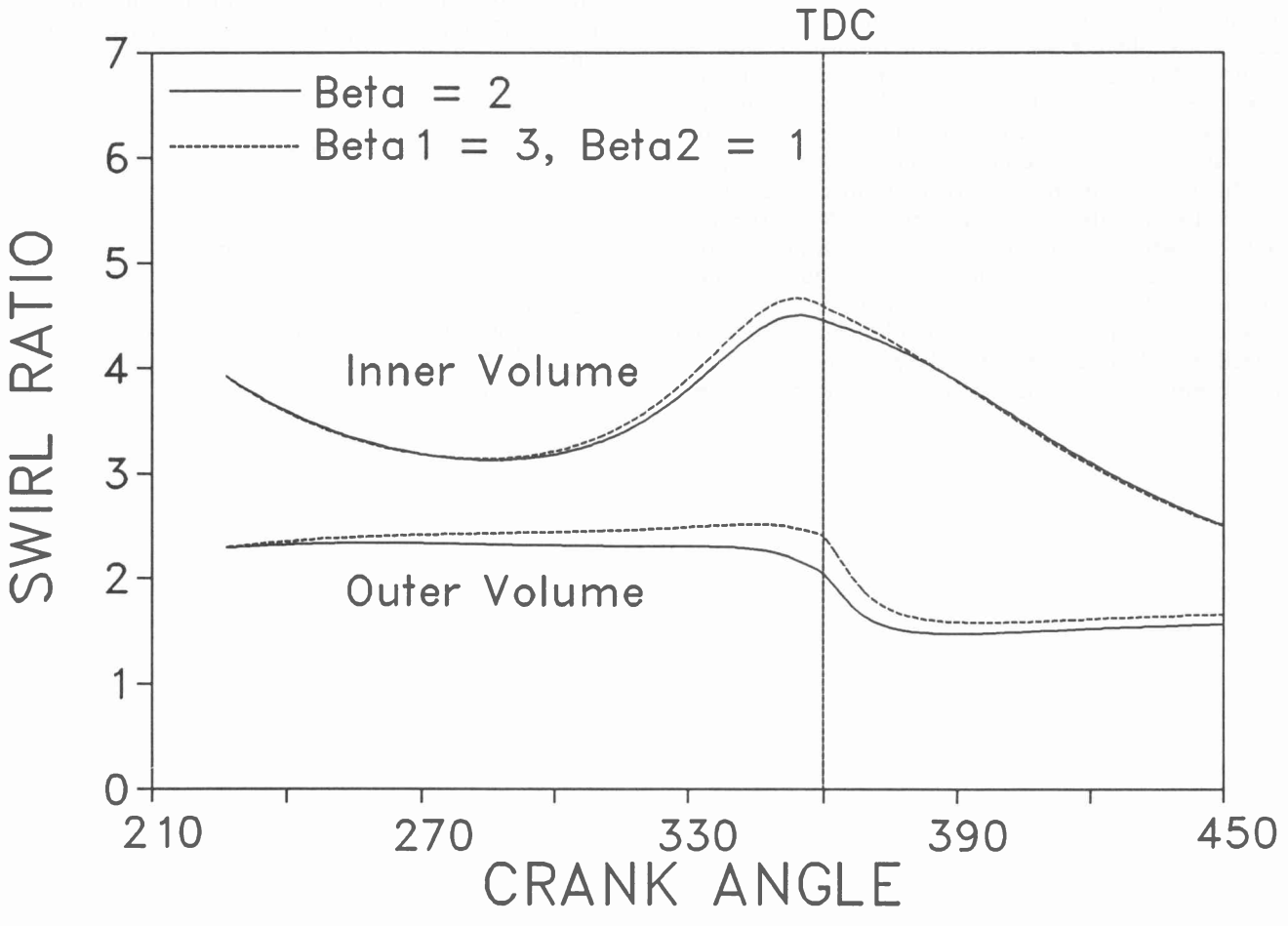

Figure 10 – The swirl ratios with different corrective coefficients for the inner and outer volumes for the standard engine of Murakami *et al.* [2].

On the basis of the good agreement obtained between the present model and the experimental data from the two very different engines of Johnston *et al.* [3] and Murakami *et al.* [2] as well as the output from the relatively sophisticated model of Morel and Keribar [4], it was concluded that the swirl ratios that were being generated by the present model were sufficiently accurate to provide a reliable foundation for the calculation of convective heat transfer. This model also provided a useful tool for investigating the effects of varying combustion chamber geometry on the gas flow processes.

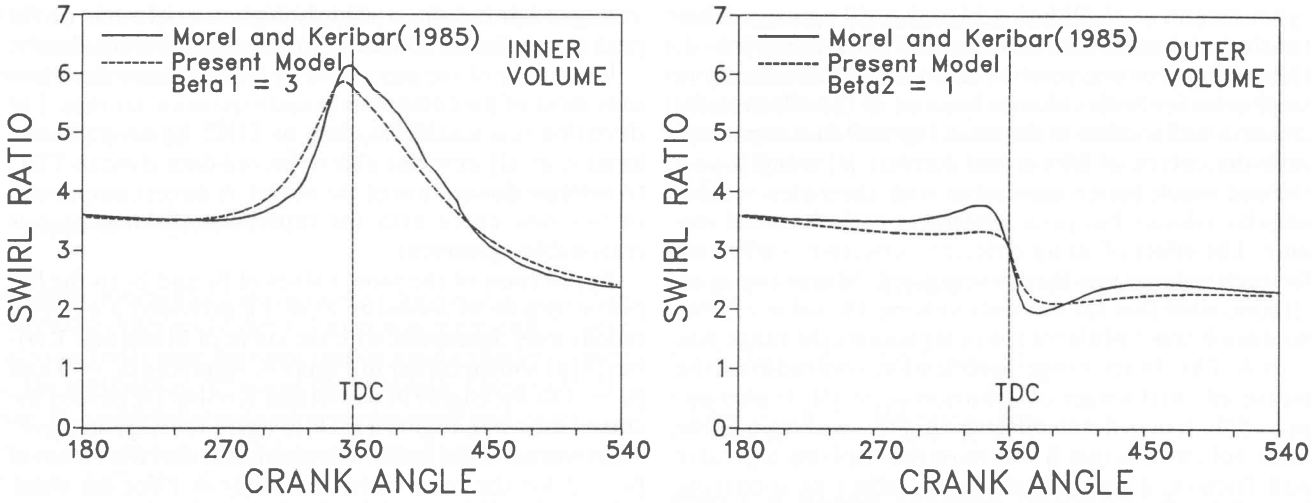

Figure 11 – The swirl ratios with corrective coefficients $\beta_1 = 3$ and $\beta_2 = 1$ as compared to the model output of Morel and Keribar [4].

Conclusions

In the calibration and verification of the gas flow processes, excellent agreement with published data was achieved for the squish and swirl components of gas flow generated by the model. In addition these results were obtained for both a bowl-in-piston engine configuration typical of direct injection diesel engines and a flat piston configuration typical of spark ignition engines. It was concluded that the model was able to predict the dominant gas velocity components of squish and swirl for a broad range of engines with a precision that would provide a firm foundation for the calculation of convective heat transfer rates. This model could also be used as an effective tool for investigating the consequences of varying combustion chamber geometry on the gas flow processes. While emphasis was placed on diesel engine configurations, the model could be adapted easily for analysing swirl and squish processes in spark-ignition engines.

References

1. Arcoumanis, C. and Whitelaw, J. H., 1987. Fluid mechanics of internal combustion engines – a review. Proc. I. Mech. E., 201 (C1): 57-74.

2. Murakami, A., Arai, M. and Hiroyasu, H., 1988. Swirl measurements and modelling in direct injection diesel engines. SAE paper 880385.

3. Johnston, S. C., Robinson, C. W., Rorke, W. S., Smith, J. R. and Witze, P. O., 1979. Application of laser diagnostics to an injected engine. SAE paper 790092.

4. Morel, T. and Keribar, R., 1985. A model for predicting spatially and time resolved convective heat transfer in bowl-in-piston combustion chambers. Trans. SAE paper 850204, 94: 2.77–2.93.

5. Goering, C. E., 1986. Engine and tractor power. PWS Publishers, Boston, Massachusetts, USA.